Research Article

Monika Kroneberger*, Andreas Mezger and Stephanie Becker

Stray light and ghosts in catadioptric spectrometers: incorporating grating scatter measurements into simulations and ghost sensitivity into system design

https://doi.org/10.1515/aot-2018-0039
Received August 3, 2018; accepted October 22, 2018; previously published online November 22, 2018

Abstract: The accurate simulation of stray light is essential for the verification of the contrast requirements in optical instruments. In a spectrometer, the scattering from reflective gratings is difficult to characterize while contributing significantly to the overall system stray light and reduction of the spectrometer contrast. In addition, the multiple diffraction orders create a ghost sensitive environment, which must be considered in the design of the instrument. In this article, we present an experimental setup for, and measurement results from, the characterization of the bidirectional scattering distribution function (BSDF) of a holographic grating for a spectrometer applied in a typical earth observation mission with demanding stray light requirements. We observed distinct stray light peaks out of the diffraction plane, which are called 'satellites.' The main challenges in the measurement of grating BSDFs arise from the near angle limit, the determination of the instrument signature and the selection of the appropriate sampling (2D or 3D). Following the grating characterization, the next step is to introduce these measured BSDFs into stray light simulation. We have done that by fitting appropriate functions to the measured BSDF and defining them in the optical analysis software ASAP as a user-defined BSDF. Ghost analysis is done at the spectrometer level as a sensitivity analysis of the tilts of the optical elements. Due to the ghosting of higher diffraction orders of the grating, a high sensitivity to the tilts of some of the optical elements can be seen.

***Corresponding author: Monika Kroneberger,** OHB System AG, Optical Department, Manfred-Fuchs-Straße 1, 82234 Weßling, Germany, e-mail: monika.kroneberger@ohb.de. www.ohb.de
http://orcid.org/0000-0002-4291-6418
Andreas Mezger and Stephanie Becker: OHB System AG, Optical Department, Manfred-Fuchs-Straße 1, 82234 Weßling, Germany

Keywords: BSDF; ghost analysis; optical gratings; spectrometer; stray light.

1 Scatter measurement and simulation

1.1 Introduction

The stray light requirements for the spectrometer gratings are defined in terms of equivalent surface roughness [1]. The required BSDF is approximated by a Harvey-Shack function (see Figure 1) at the peak of the diffraction order at which the grating is designed to operate. The BSDF function measured by a scatterometer, such as the Albatross TT, is expressed by the following equation, corresponding to the geometry illustrated one in Figure 2:

$$\mathrm{BSDF}\left(\theta_i,\theta_s,\phi_s\right)=\frac{dP_s\left(\theta_i,\theta_s,\phi_s\right)}{d\Omega_s P_i\cos\theta_s},$$

where θ_i is the incident angle; θ_s and ϕ_s refer to the azimuthal and tangential scattering angles, respectively; P_i is the power incident on the sample; and P_s is the scattered power collected by the detector in the solid angle $d\Omega_s$.

This setup allows the measurement of a 3-dimensional (3D) bidirectional scattering distribution function (BSDF) by varying θ_s and ϕ_s for a given incidence angle. The properties of the Albatross TT are summarized in Table 1. The near angle limit is defined by the angle from the center of a reflection peak, where the scatterometer is able to determine between instrument signature and stray light from the test sample. The near angle limit depends on the optical geometry of the scatterometer and the sample under test. The instrument signature is the BSDF of the scatterometer itself.

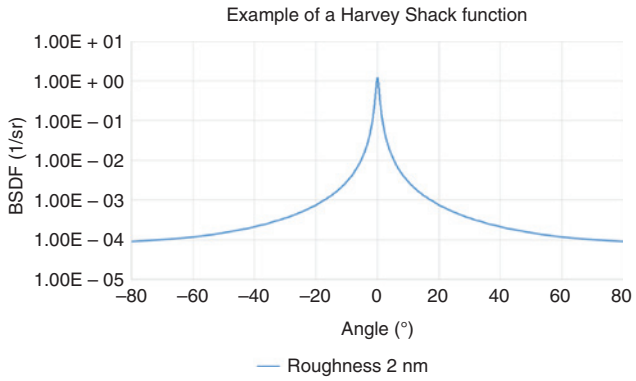

Figure 1: Example of a BSDF approximated by a Harvey-Shack function for a mirror with 2 nm roughness at 532 nm wavelength.

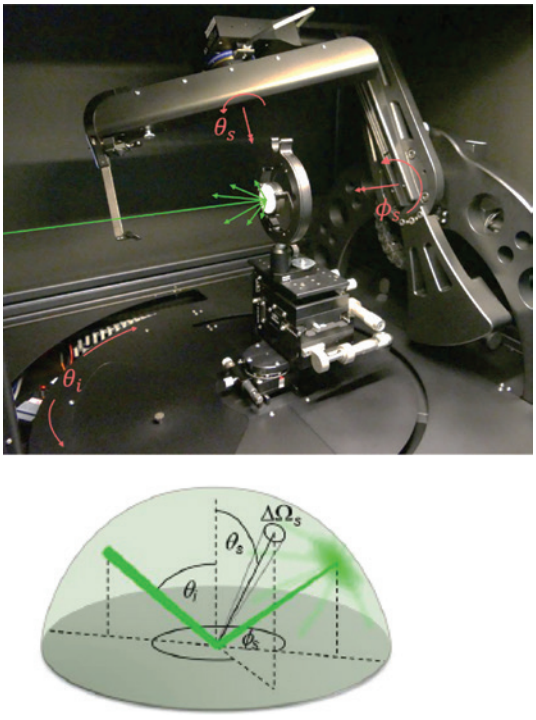

Figure 2: Albatross TT and its measurement geometry (right figure extracted from the manual courtesy of Fraunhofer IOF).

Table 1: Albatross TT properties.

Albatross TT	
Wavelength	532 or 1064 nm
θ_i	−90° to +90°
ϕ_s	−90° to +90°
θ_s	−180° to +180°
Angular resolution	<0.02°
Dynamic range	13 orders of magnitude
Near angle limit	0.1°
Sample size	<100 × 100 mm

1.2 Measurement of the curved samples

The gratings used in the Offner-type spectrometers for earth observation are spherical or weakly aspherical to improve the optical performance of the spectrometers and have a convex shape. To measure the curved gratings, we need to focus the scatterometer. In the nominal setup, the beam is focused on the detector [5]. With a non-flat sample, a refocusing has to be done to achieve again the focus on the detector. Focusing is achieved by adjusting the focusing unit of the scatterometer's 'beam preparation unit.'

Once focused, we cannot use the setup without a sample with an appropriate curvature. This makes it impossible to take the direct measurement of the scatterometer's signature without a sample. In our case, we are interested in the near-angle signature, which includes aberration and stray light from the scatterometer optics. There are two ways to obtain the near angle signature in a focused configuration.

1.2.1 Indirect method

1. First, the signature measurement is done in a standard configuration (appropriate for flat samples).
2. Then the signature is simulated, including the stray light and aberration in the same configuration, to a reasonable agreement with the measured signature. A critical aspect is to model correctly the stray light properties of all components (Figure 3 (top)).
3. The simulation is re-done in the focused configuration (appropriate for the curvature of interest). As the scattering properties of the optical elements do not change and we simulated the sample as a perfect mirror, our simulation in Figure 3 (bottom) should be close to the real instrument signature for a convex sample curvature of 100 mm.

1.2.2 Direct method

It is also possible to replace the sample by a mirror with the same curvature and negligible scattering behavior. Next, the BSDF we measure is very close to the real instrument signature (see Figure 4).

The simulated near-angle signature is a combination of three contributors: optical aberrations in the scatterometer (or in the combination of scatterometer and sample in the focused case), scattering from the instrument itself and clipping by the detector field of view.

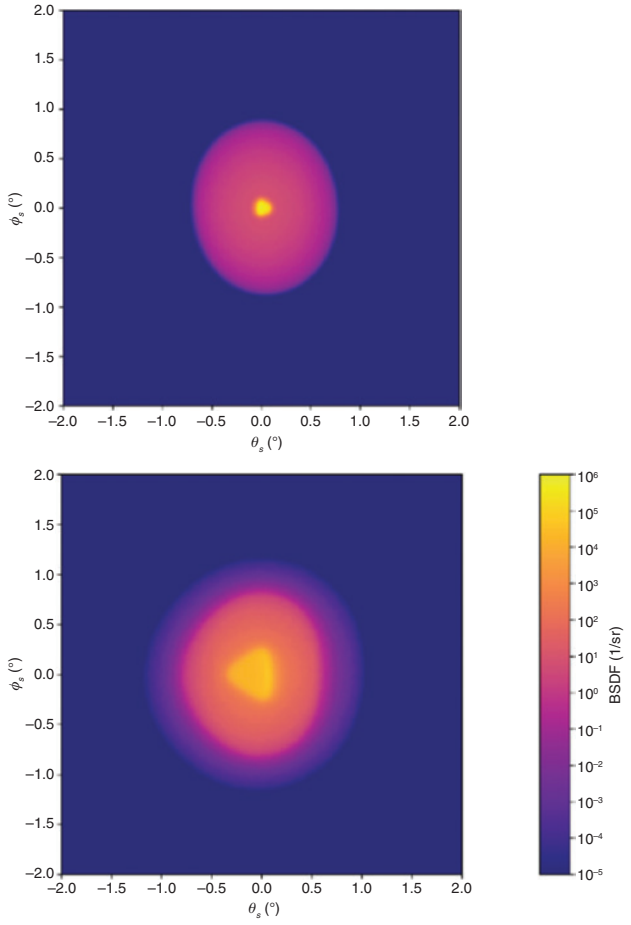

Figure 3: Top: Simulated scatterometer near-angle signature for the nominal configuration. This simulated irradiance pattern is in good agreement with the measurements illustrated in Figure 4. Bottom: Simulation of a focused configuration adapted for a convex sample with a 100-mm radius of curvature.

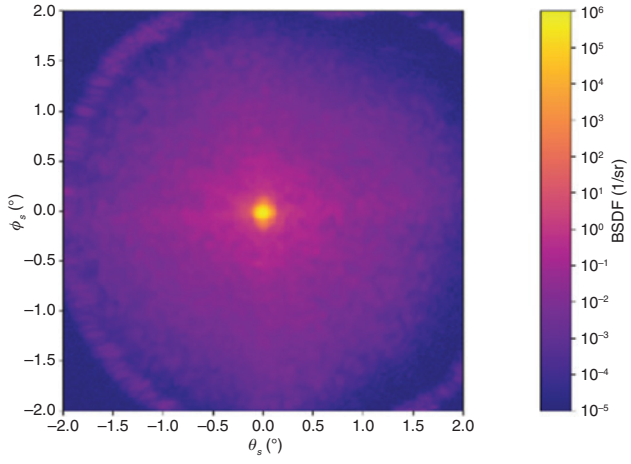

Figure 4: Measured scatterometer near-angle signature for the nominal system.

In the focused case, the aberration increases reciprocally with the convex radius of curvature of the test sample and the near angle limit occurring already between 0.5° and 0.7° instead of 0.1° in the nominal configuration. These results also illustrate a limitation of the measurement setup, namely, the impossibility of measuring scattering close to the specular direction (within the near angle limit) due to the width of the signature function.

The simulation of the nominal configuration does not match the measurements, especially between 0.1° and 0.6°, where the scattering of the scatterometer optics is dominating the near-angle signature. For our stray light simulation, we used the parameters given in [2] for the Albatross TT; however, we expect that these values are somewhat pessimistic and that the Albatross TT system exhibits lower stray light levels.

For a comparison with our grating measurement, we used an off-the-shelf silicon lens as a mirror in reflection, with the same radius of curvature as the grating. For each grating curvature, the matching lens or mirror has to be used. We found that optical aberrations dominate the instrument signature. For the grating under investigation, the angular range was up to 0.6°–0.7°. Figure 5 shows the BSDF around the –1st order diffraction peak of the grating and the instrument signature BSDF obtained by substituting the silicon lens for the grating. To account for the different values of reflectivity and grating efficiency, we scaled the signature BSDF to give the same value at the peak. The lens has a non-negligible roughness enlarging the scatter and giving some sort of upper limit signature.

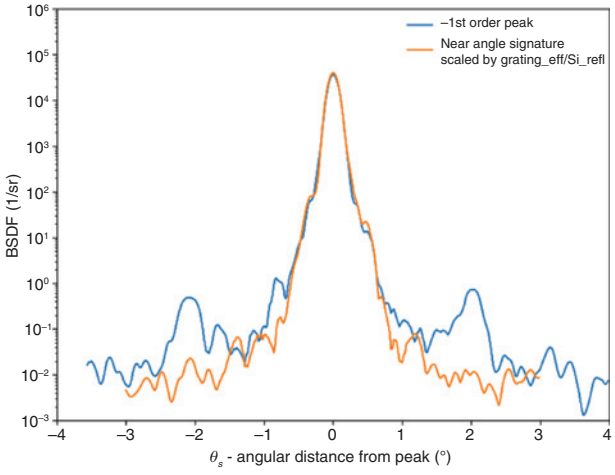

Figure 5: Comparison of the –1st order peak scattering of a convex grating and measured instrument signature, making use of a silicon lens with same curvature. The FWHM of the signature is determined by the aberration of the scatterometer plus the sample curvature. Contributions below 10^0 1/sr are determined by the scattering properties.

The angle where the signature drops below the measured signal defines the near-angle limit for the specific measurement. For smaller angles, it cannot be discriminated if the measured signal is part of the system signature or if it is a real signal from the sample under test. In the setup for the grating under investigation (Figure 5) the near angle limit is 0.6°.

1.3 Measurement results

Measuring the two-dimensional (2D) BSDF of the grating and comparing it to the calculated BSDF for several roughness values fitted with a Harvey-Shack formula [3, 4] shows that the grating scattering is lower than an equivalent 2 nm RMS roughness scattering BSDF above 1° scatter angle. However, as indicated in Figure 6, two features stand out of the envelope curve. From the 2D plot, it is difficult to determine whether the features are point-like or ring-like in the angular domain.

Using the Albatross TT, we are able to measure a 3D scan (Figure 7), indicating that the features form scattering rings and other peaks around the diffraction peaks. Out of the full 3D scan, we show only the vicinity of the nominal diffraction peak at the –1st order. The cut-line in Figure 7 marks the angles measured with a 2D scan (Figure 6). This line clearly hits the maxima of the satellites but only by chance.

Furthermore, at each location on the grating, the BSDF can be different. The scatter map for the actual item under test at two different measurement positions on the grating surface (again only the vicinity of the –1st (nominal) diffraction order) shows variations in the positions and sizes of the features (see Figures 8 and 9).

The measured results emphasize the importance of 3D scanning when measuring a grating's BSDF. Restricting the measurement to 2D would produce different results depending on the alignment of the measurement plane with respect to the diffraction plane. The position of the

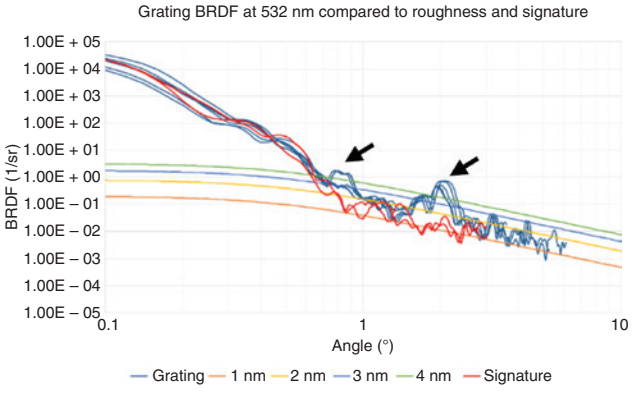

Figure 6: Grating BSDF compared to roughness BSDF, features of interest are indicated by arrows.

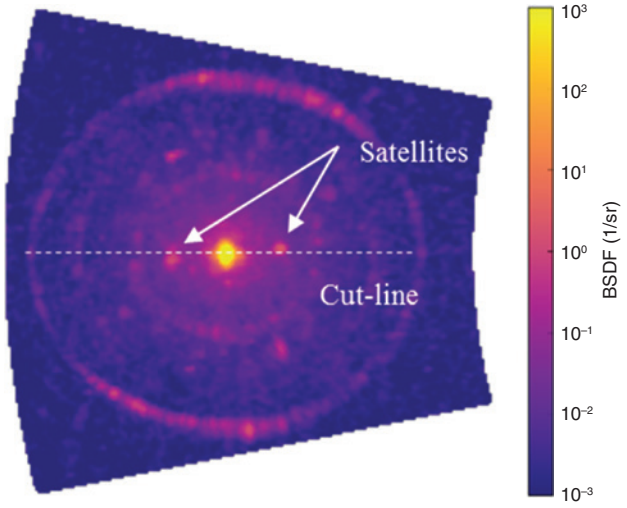

Figure 7: 3D BSDF map of the grating at the –1st order peak (range φ_s=–13°–13° and θ_s=–43.4°–25.4°) feature showing the angle of the satellites.

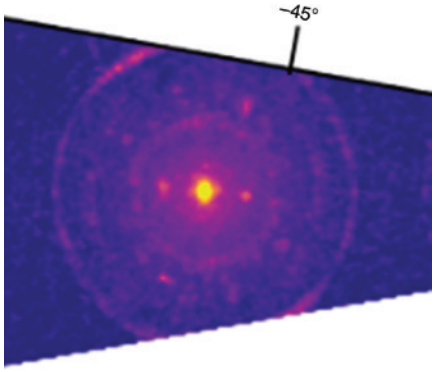

Figure 8: 3D BSDF map for the second location on the grating for scatter angles roughly between –43° and –25° and ±10°.

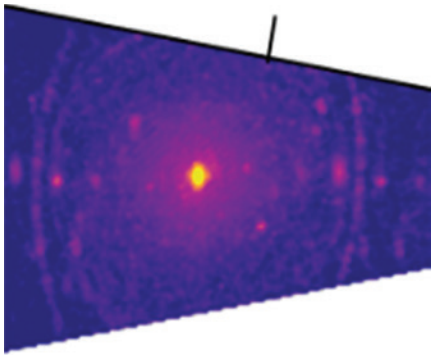

Figure 9: 3D BSDF map for third locations on the grating for scatter angles roughly between –43° and –25° and ±10°.

satellites is a local property of the grating, which cannot be measured reliably with a 2D scan.

1.4 Simulation results with the analytical grating BSDF

The BSDF was finally applied to the simulation of the complete spectrometer system. We chose to fit the satellites with Gaussian functions and the smooth scattered light with a Harvey Shack function [6]. The following simulation is for one BSDF (one surface location) only. For a better system analysis, multiple surface points must be averaged and then the structures fitted. The simulation considers the roughness scatter on all optical elements, but contamination and ghosting from other optical elements are not considered. The wavelength 500 nm was chosen (the lowest wavelength of the detection range). Figure 10 shows the resulting stray light in the detector plane of the spectrometer on top of the nominal image of a point source. In addition to the halo around the image of the point source (top center of Figure 10), the satellites of the grating as scatter are clearly visible. In a nominal scene, they will add to the spectral and spatial stray light, because they are displaced from the image of the source in both directions. The relative irradiance with respect to the nominal light is of the order 10^{-6} and will normally not disturb a scene significantly. However, for high-contrast scenes (for example with clouds and earth surface), the nominal illumination can vary by one to two orders of magnitude from line to line and cause the relative irradiance to be significantly increased. As the stray light requirements for spectrometers for earth observations can be in the range of 10^{-4}, we conclude that the satellites of gratings can lead to the non-compliance of the instrument to the requirements. The presented simulations are performed exemplarily and are valid only for a small sub-aperture of the grating, where we measured the underlying BSDF. As the BSDF may depend on the position at the grating surface, the final image can be smeared out and even more satellites could appear.

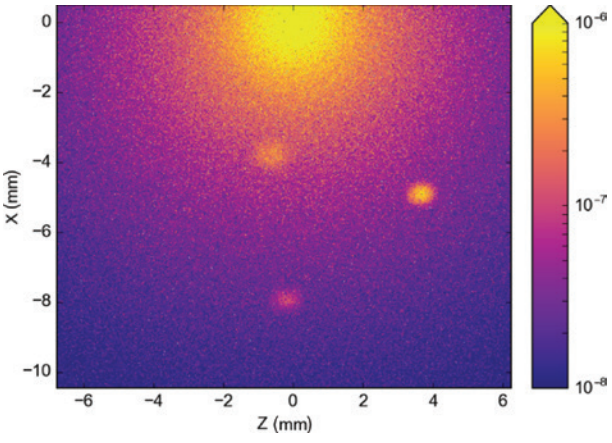

Figure 10: Roughness scatter distribution on the detector for a point source of 500 nm in the middle of the spectrometers slit.

1.5 Requirement definition for the grating suppliers

The measurement and simulation of the grating BSDF have shown that the satellites can travel through the system and cause stray light on the detector. The challenge now is to define the requirements for the grating to minimize these satellites. In case of a holographic manufacturing of the grating, the process allows the minimization of the amplitude of the superimposed structures, and even the adjustment of their period. In that way, we can influence the location of the satellites at the detector plane. Given that superimposed structures are a matter of optimization and their relation to satellites is predictable, we propose to define an exclusion zone for satellites (red rectangle in Figure 11). Furthermore, we propose to keep the existing requirement definition of a maximum equivalent rms roughness in the form of a maximum BSDF template, as illustrated in Figure 11. If some satellites still occur inside the specified exclusion zone, their intensity is required to be below the specified BSDF template. Outside the exclusion zone, the satellites can be ignored.

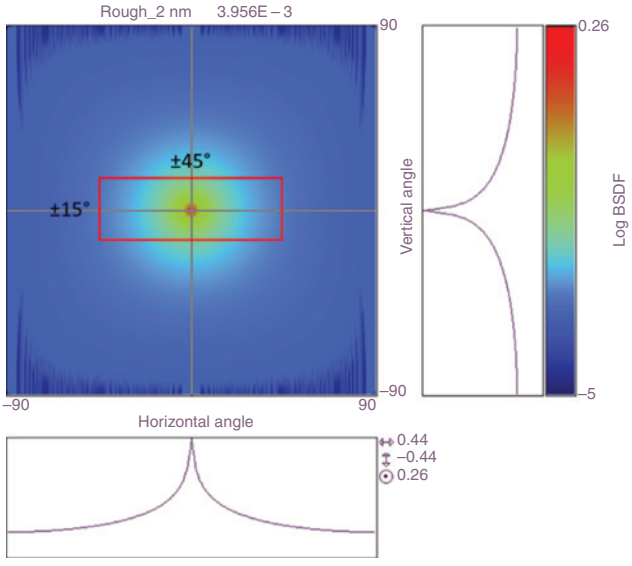

Figure 11: BSDF template for the grating scatter and exclusion zone for satellites. (Dark lines are artefacts from translation into rectangular angle space).

In order to achieve an independently verifiable requirement, we propose to define the exclusion zone and BSDF template in the angle space. The grating of a spectrometer is located at the pupil of the system. Therefore, we can exploit the Fourier relationship between the pupil and image space.

The exclusion zone shall consider the spectral and spatial limits of the detector, because the diffraction pattern shown in Figure 10 shifts across the detector plane with different image points in the slit and different wavelengths. The scatterometer illuminates only a small spot of less than 1 mm diameter on the grating. When changing the position of this spot on the gratings surface, we observed a variation of the satellite in position and intensity as an effect of surface irregularities as described in Section 1.3. We need to consider this during the verification of our requirement. Thus, an adequate number of measurement positions and a consistent averaging of the results is required to correctly predict the stray light performance on system level, where the full clear aperture of the grating is illuminated.

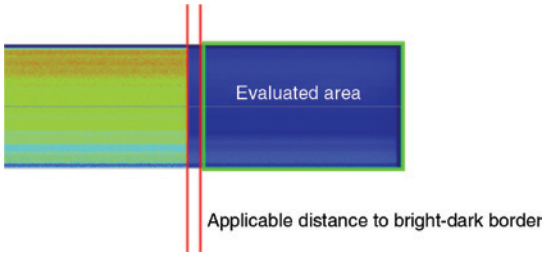

Figure 12: Example for a half-field illumination for an earth observing instrument for stray light analysis.

the other half with a low irradiance comparing to a scene with a cloud in the field of view (see Figure 12). The stray light is then specified in the dark half of the detector with an exclusion zone defined by a distance to the bright dark border.

The in-field light from the bright half of the slit can give rise to ghosts detected in the image of the dark half of the slit. These ghosts appear to be spectral signals from the scene, contaminating the true spectral signal.

2 Ghost sensitivity analysis on spectrometer level

2.1 Introduction

Another source for the performance reduction of a spectrometer from the straylight point of view are the ghosts. When gratings are used as diffractive elements, the higher diffraction orders add to the system ghosts. While designing the spectrometer, care has to be taken to guide those into directions not pointing towards the detector or to block them with baffles if possible. When the higher diffraction orders reach other optical elements, they will add to the ghosting in the system.

A week point in the stray light simulation is the fact that mostly nominal systems are analyzed. For the scattered light, the results for the nominal and the as-built system will mostly only differ slightly. Ghosting, however, is strongly dependent on the actual detailed optical set-up of the instrument. Moreover, due to the manufacturing tolerances and alignment shifts and tilts, smaller as-built variations might have a significant influence, depending on the set-up.

In earth-observing instruments, the stray light requirement is often defined by a half field scene, where half of the source is illuminated with a high irradiance,

2.2 Simulation of an Offner type spectrometer

We did a sensitivity analysis for the alignment tolerances of the optical elements to specify the worst offenders to ghosting. The optical components were tilted individually by +/ – 1° in the x- and y-directions (local element coordinate system, x in Figure 13 is always perpendicular to the picture plane, y is parallel to picture plane). The high values for tilt were chosen to obtain a significant effect and easy identification of the worst offenders. In Figure 13, the nominal and parasitic ray paths of the analyzed system are depicted.

One spot in the middle of the slit and seven equally spaced wavelengths in the range of the spectrometer were simulated. The sensitivity check consisted of the test cases listed in Table 2. We generated a slightly oversized detector area for the 45 × 13 mm flight detector size, to get an idea of all the occurring ghost and where they originate. This can be important in ensuring compliance to the requirement. The nominal light of the spectrometer, which is illustrated in Figure 14, corresponds to the nominal performance without any stray light.

In Figure 15, the ghosting of the nominal optical system is shown. The dark intense dots still represent the nominal spectrometer image. The larger week ghost areas are negligible. The small intense areas beside the intense

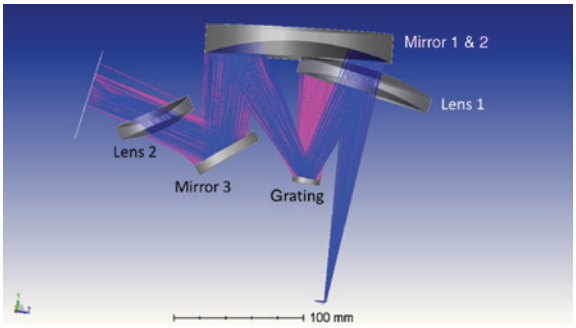

Figure 13: Nominal ray path (blue) and parasitic path (pink).

Table 2: Investigated displacements (the columns were simulated in separate runs).

Element	Tilt x [°]	Tilt y [°]
Lens 1	1	1
Mirror 1 & 2	1	1
Grating	1	1
Mirror 3	1	1
Lens 2	1	1
Lens 1		1
Mirror 1 & 2		1
Lens 1		−1
Mirror 1 & 2		1

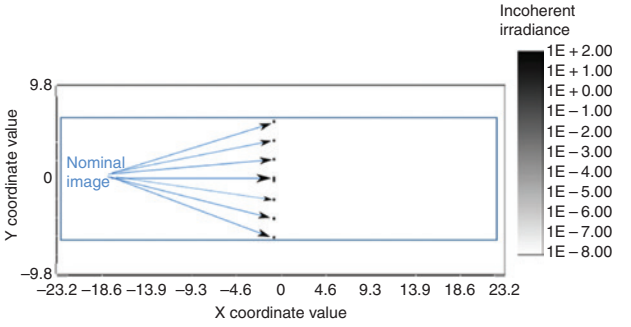

Figure 14: Direct light of the point source (seven wavelengths simulated) of the nominal design of the spectrometer (the blue rectangle is the flight detector area).

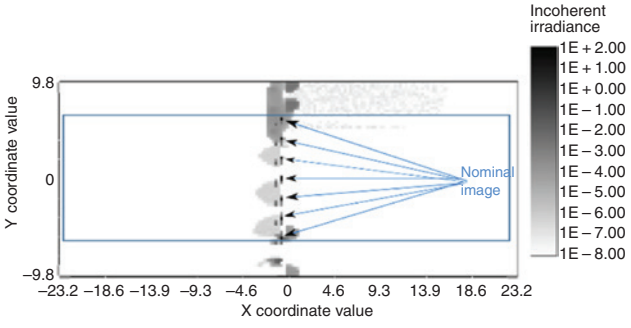

Figure 15: Direct light with ghosts in the nominal configuration.

dots of the nominal image contribute significantly to the overall stray light.

The sensitivity study shows that the first three elements of the examined spectrometer, as depicted in Figure 13, are critical. In particular, these elements are Lens 1 of the combined mirror Mirror 1 & 2 and the grating. In Figure 16, the shifting of the ghosts to other field positions on the detector level due to a tilt of 1° in y-direction of Lens 1 can be observed.

In Figure 17, the result of a tilt of 1° in the y-direction of Mirror 1 & 2 is depicted. This tilt causes a shift of the nominal image and a shift of the ghosts to both sides of the nominal image. In Figure 18, the resulting image of a tilt of the grating can be seen. In comparison to the tilted mirror or lens the image stays almost at the same location and the ghosts move to the other side but show less shift. In Figure 19, the influence on the image of a combined tilt two elements can be observed. The nominal image is displaced and the ghosts are shifted to both sides as well.

The sensitivity study shows that a knowledge of the imaging and stray light performance of a nominal optical system is not enough to perform an accurate stray light analysis. If the sensitivity on ghosting of the optical elements is not taken into account, the system might become non-compliant to the requirement due to ghost images on the detector.

Looking at the paths contributing to the shifted ghost spots, they all originate at the +1st diffraction of the grating (the –1st being the nominal order). The light goes back to Lens 1 and Mirror 1 & 2 and then back through the full system using the –2nd diffraction order at the grating to propagate to the detector (see Figure 20). In this special design, there is almost no possibility to block those rays.

Optimizing a design for ghosting is possible and should be done as early as possible in the spectrometer conceptual design phase. In this case, removing Lens 1 reduces ghosts by an order of magnitude and the sensitivity is much smaller. Figure 21 shows the resulting ray paths. The remaining ghost paths with the involvement of the grating again use the +1st and –2nd diffraction orders.

Figure 22 shows the ghosts of the nominal configuration of the optimized design. Only large-area and low-intensity ghosts are visible. In Figure 23, the result of a tilt of 1° in the y-direction of Mirror 1 & 2 is depicted. This tilt causes a shift of the nominal image and a shift of the ghosts. Ghost intensity is lower than that in the first design. In Figure 24, the resulting image of a tilt of the grating can be seen. Again, the image stays almost at the same location and the ghosts move to the other side but with low intensities.

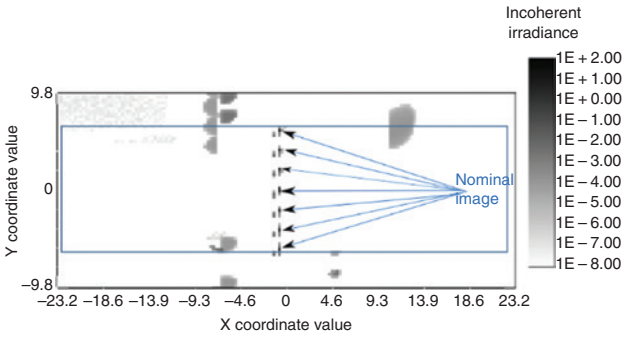

Figure 16: Tilt of 1° in the y-direction of Lens 1.

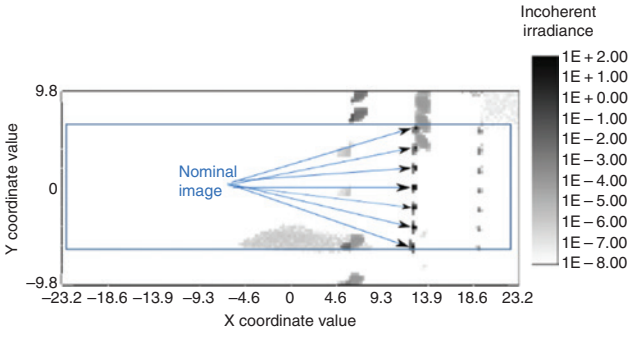

Figure 17: Tilt of 1° in the y-direction of Mirror 1 & 2.

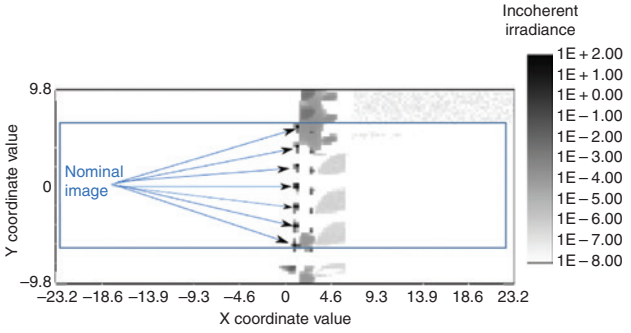

Figure 18: Tilt of 1° in the y-direction of the grating.

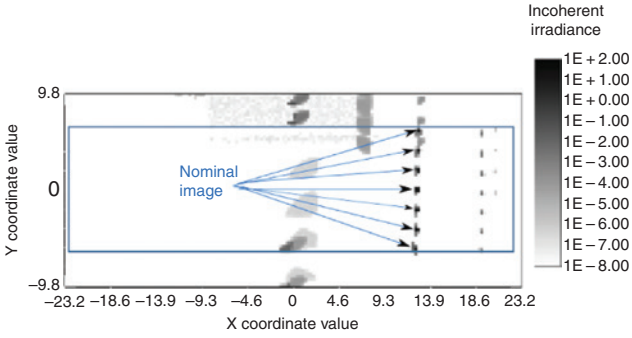

Figure 19: Combined M1+M2 tilted by 1° and L1 by –1° in the y-direction.

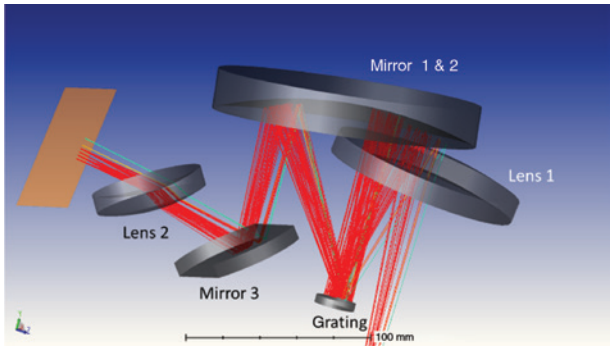

Figure 20: Ghost path of the shifted ghost spots with the tilted first mirror. The rays are colored by wavelength.

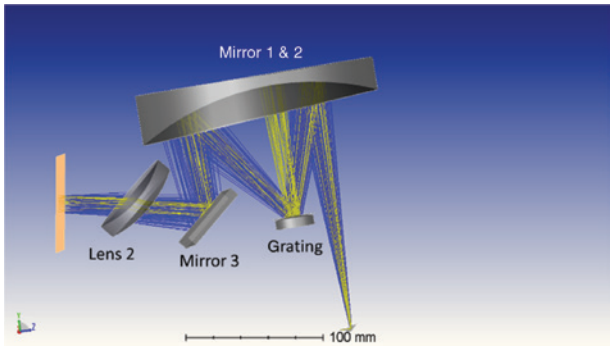

Figure 21: Nominal ray path (blue) and parasitic path (yellow) for the optimized system.

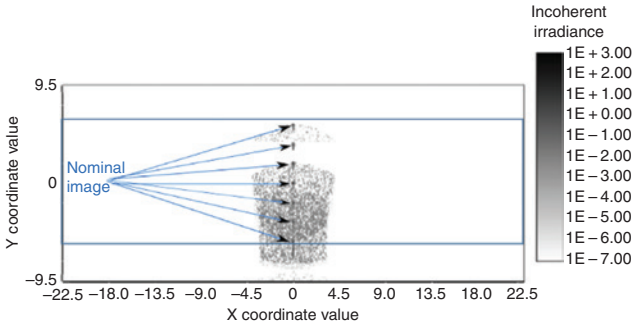

Figure 22: Optimized design ghosts in the nominal configuration.

2.3 Result of the sensitivity analysis

The result of the ghost sensitivity analysis for the spectrometer under investigation is a high sensitivity of Mirror 1 & 2 and a medium sensitivity of the grating for tilts around the local y-axes. Both designs showed this sensitivity but the optimized design reduced the ghosting effect significantly. Lens 1 was detected as the worst offender in ghosting and thus a removal had been investigated.

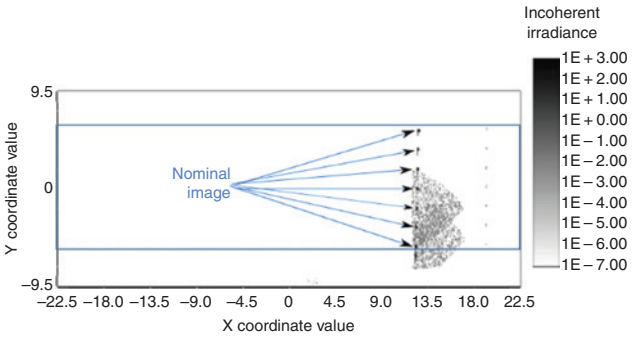

Figure 23: Optimized design, tilt of 1° in y-direction of Mirror 1 & 2.

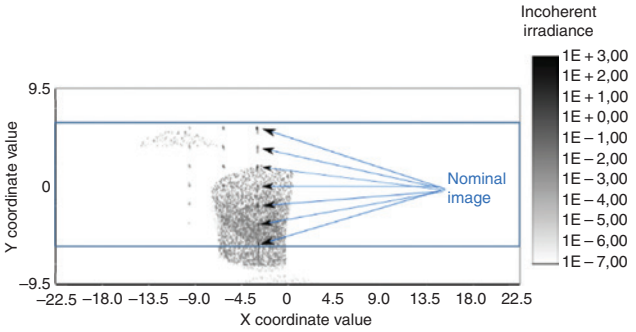

Figure 24: Optimized design, tilt of 1° in y-direction of grating.

An interesting observation can be made upon comparing the worst offenders of a standard type optical performance and tolerance analysis. The tolerance analysis found as worst offenders with respect to tilts are as follows: tilt x of grating and tilt x of Mirror 1 & 2. The y-tilt is not in the first 30 entries of the sorted list of offenders. These results show that, for the performance and assembly strategy of the instrument, not only a tolerance analysis for optical performance is necessary but also a ghost sensitivity analysis.

The design of the system and the design of the grating define the stray light sensitivity of the system individually. No prediction before the design is possible, and a analysis has to be done for each design.

3 Conclusion

We have shown the importance of characterizing BSDF with 3D scanning methods when studying highly anisotropic components, such as gratings. The setup used in this article is capable of such measurements. It is insensitive to misalignment between the scanning plane and the diffraction plane that other measurement setups might have.

Proper care was taken to characterize the scatterometer signature, as the use with convex samples do not allow a direct measurement of that signature. In particular, we investigated the determination of the near-angle limit in our measurements, because of its inverse relationship with the radius of the curvature of the grating. Simulations of the optical path showed that aberrations are the main cause of a degraded near angle limit.

A standard convex spherical blazed holographic grating was used as the test item. The grating exhibited anisotropic features in the grating BSDF caused by superimposed grating patterns on the sub-apertures of the nominal grating. These grating patterns are probably produced by false light in the illumination optics used in the production of the grating structure itself. The level of these effects can be negligible for standard spectrometers on ground, but is of significance for spectrometers used for earth observation from space and for spectrometers in other high-end applications. Therefore, the production of holographic gratings for high-end applications require a sophisticated optimization process that considers all relevant stray light aspects. These kind of effects need to be taken into account, when the detailed requirements for such gratings are being defined.

Fitting the measured BSDF with analytical functions (Gaussian peaks and Harvey-Shack functions), a BSDF of the grating for stray light simulation was explained. Our simulation shows that the satellites can have significant influence on the image at the detector. We propose a set of stray light requirements for gratings, specifying a BSDF template and an exclusion zone for satellites within a certain angular range, which corresponds to the detector dimensions.

Ghosts are a further topic in the spectrometers, which are highly related to the grating. Higher diffraction orders not only have to be blocked from directly reaching the detector but possible ghost paths with other optical elements must also be investigated. These paths can be extremely sensitive to the tilts of the optical elements. A compliant nominal system with respect to stray light performance could easily become non–compliant, by slightly tilting optical elements during alignment. A sensitivity check with two different spectrometer designs showed that, in similar designs, different optical elements can be the worst offenders for stray light. Moreover, the worst offenders of the tolerance analysis for nominal optical performance, like wavefront error, can also differ from the worst offenders found in the ghost sensitivity analysis, thus leading to additional alignment constraints.

Acknowledgements: The authors acknowledge that this work is supported by an ESA funding through the FLEX Mission development. We also wish to acknowledge the contribution of Riccardo Gabrieli of Leonardo S.p.A. in coming up with the new definition of the grating requirement.

References

[1] B. Harnisch, A. Deep, R. Vink and C. Coatantiec, “Grating Scattering BSDF and Imaging Performances”, ICSO 2012, FP 156.
[2] A. Finck, ‘Table Top System for Angle Resolved Light Scattering Measurement’, dissertation at Fakultät für Maschinenbau der Technischen Universität Ilmenau, urn:nbn:de:gbv:ilm1-2014000214 (2014).
[3] S. J. Wein, ‘Small-Angle Scatter Measurement’, PhD Theses University of Arizona (1989).
[4] M. G. Dittman, ‘Contamination Scatter Functions for Stray-Light Analysis’, Proc. SPIE Vol. 4774 (2002).
[5] M. Kroneberger and S. Fray, Adv. Opt. Techn. 6, 379–386 (2017).
[6] M. Kroneberger, A. Mezger and J.-B. Volatier, ‘Scattering from Reflective Diffraction Gratings: The Challenges of Measurement and Verification’, Proc. SPIE 10692, 106920G (2018).

Monika Kroneberger
OHB System AG, Manfred-Fuchs-Straße 1
82234 Weßling, Germany
monika.kroneberger@ohb.de

Monika Kroneberger received her diploma in Physics in 1991 from the Johann Wolfgang Goethe University in Frankfurt/Main. Currently, she is working in the domain of optical system engineering for OHB System AG. Her main topic is stray light reduction and verification in the optical systems by simulation and measurement.

Andreas Mezger
OHB System AG, Manfred-Fuchs-Straße 1
82234 Weßling, Germany

Andreas Mezger received his diploma in aerospace engineering in 2010 from the University of Stuttgart. Currently, he is working in the domain of optical mounting, metrology and validation for OHB System AG.

Stephanie Becker
OHB System AG, Manfred-Fuchs-Straße 1
82234 Weßling, Germany

Stephanie Becker received her Master of Engineering of Laser and Optic Technology in 2013 from the University of Applied Sciences in Jena. She is currently working in the domain of optical analysis and optical engineering for OHB System AG.